Jetting Liquid Marbles: Study of the Taylor Instability in Immersed Marbles

Edward Bormashenko,[1,2,a] Roman Pogreb[1], Gene Whyman[1,2], and Albina Musin[1,2]

1Ariel University Center of Samaria, Department of Physics, Research Institute, 40700, P.O.B. 3, Ariel, Israel

2Ariel University Center of Samaria, Chemical Engineering and Biotechnology Department, 40700, P.O.B. 3, Ariel, Israel

a)Author to whom correspondence should be addressed. Electronic mail: edward@ariel.ac.il

ABSTRACT

Liquid marbles encapsulated with powders, immersed in oil and exposed to DC field were investigated. At the critical electric field, the Taylor instability of the marble arose, accompanied with a cone appearance and jetting a small droplet. The squared critical field was linear in the inverse size parameter of the marble, extrapolation of which to zero field gave a finite value (the Rayleigh limit), i.e. some marbles were charged. Lycopodium marbles and water droplet remained neutral. Therefore, charging marbles is determined by their powder coverage. The effective surface tensions at marble-oil interfaces were obtained and checked with the capillary rise method.

INTRODUCTION

Liquid marbles introduced by P. Aussillous and D. Quéré in 2001 are non-stick droplets coated with micrometrically scaled solid particles.[1] Since then, liquid marbles have given rise to the intensive experimental research.[1–29]. The state-of- art in the emerging field of liquid marbles was summarized in recent reviews.[24, 25] One of the most studied topics is actuation of liquid marbles with electric and magnetic fields important in view of their microfluidics applications.[6-8, 17, 29-33] It was demonstrated that liquid marbles may be displaced, deformed and oriented with electric and magnetic fields.[31-33]

It was shown recently that liquid marbles remain stable in surrounding liquid bringing into existence Pickering-like emulsions.[34] The present work demonstrates that water marbles immersed in organic oil could be actuated with the electric field and when it surmounts the threshold value they jet manifesting the Taylor instability.

For encapsulating the marbles 3 kinds of hydrophobic powders were used: polyvinylidene fluoride (PVDF) powder (the average diameter of 130 nm), polytetrafluoroethylene (PTFE) powder (the average diameter of 1 μm), both supplied by Aldrich; lycopodium (the diameter of particles of about 30 μm) supplied by Fluka.

The marbles and water droplets were immersed into the silicon oil (polydimethylsiloxane, Dow Corning 200, liquid with a density of 0.970 g/cm^3, viscosity of 0.34 Pa·s, and dielectric constant of 2.8). Water droplets were used for the calibration of the method presented below.

For better visualization of marbles' shapes in the electric field, the solution of $KMnO_4$ in distilled water was added. This gave rise to the solution with the resistivity of 15 kΩ/cm (DC), the resistivity of pure water being 1.5 MΩ/cm, as measured with MT 4090 LCR Meter (MOTECH).

The scheme of the experimental unit used for electrostatic actuation of marbles is presented in Figure 1. Liquid marbles were immersed into the cuvette with the height of 1.5 cm filled with silicon oil and sank to the bottom. Two metallic plates were attached to the cuvette. The DC voltage was applied to the plates, and the uniform electric field was created between them. Power supply Pasco, model SF-9586, was used with the voltage range of 0–10 kV.

The experiment was carried out as follows. First, the negative pole of the power supply was connected to the upper electrode, and a voltage was raised slowly. The marble was deformed, in some cases it rose slowly and sank again. This step lasted for approximately 2 min. When a marble settled on the bottom, the voltage polarity was switched fast (in 2-3 s).

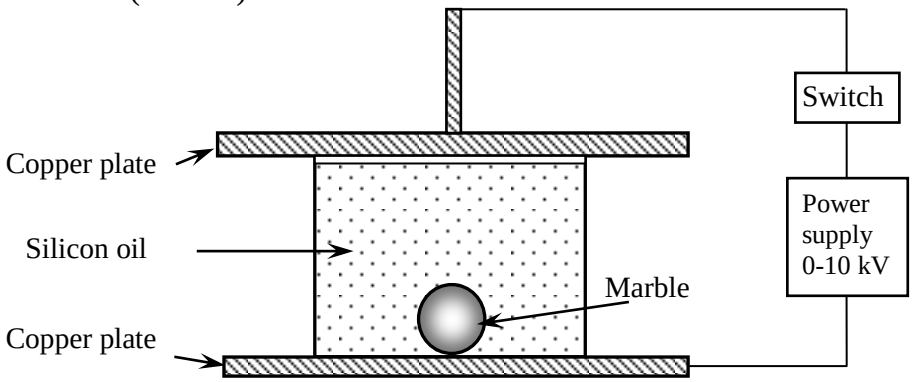

FIG. 1. Scheme of the experimental unit used for electrostatic actuation of marbles.

The behavior of marbles and water droplets under increasing DC voltage is illustrated with Figures 2 and 3. First they were deformed as depicted in Figures 2(a) and 3(a). At some critical value of electric field, E_c, the Taylor cone was formed at the upper end of a marble directed towards the positive electrode (see Figures 2(b), 3(b)) followed by jetting a small droplet (Figures 2(c), 3(c)). Pictures were taken with the rapid camera Casio Exilim 40 fps.

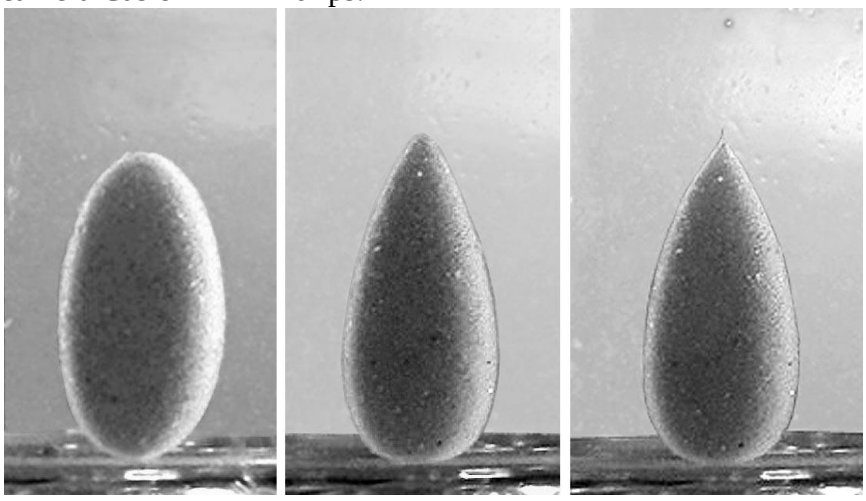

(a) (b) (c)

FIG. 2. Lycopodium-coated marble deformed in the electrostatic field of $0.48 \cdot 10^6$ V/m to the prolate-spheroid shape (a). The Taylor cone formation at the end of marble (b) followed by jetting (c) at the field value $0.51 \cdot 10^6$ V/m. Volume of the marble was 20 μl.

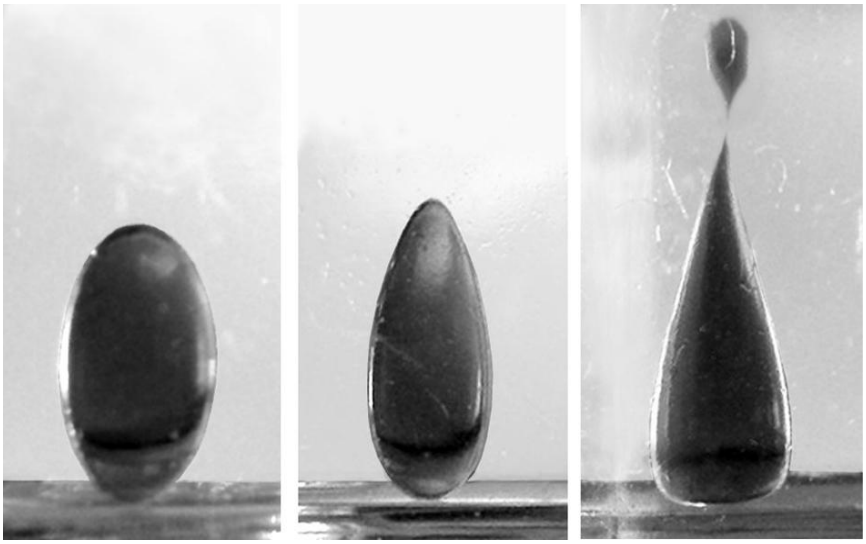

(a) (b) (c)

FIG. 3. Water droplet deformed in the electrostatic field of $0.41 \cdot 10^6$ V/m to the prolate-spheroid shape (a). The Taylor cone formation (b) followed by jetting (c) at the field value of $0.42 \cdot 10^6$ V/m. Volume of the droplet was 20 μl.

The critical electric field, E_c, measured immediately prior to the appearance of the Taylor cone (Figures 2(a), 3(a)) is presented graphically in Figure 4 in a form of the dependence of E_c^2 versus the inverse radius $1/r_0$ of the spherical marble of equal volume. Each point was averaged over 8 measurements. This dependence has a linear form

$$E_c^2 = A\frac{1}{r_0} + B\,. \tag{1}$$

Equation (1) reflects the balance of the electrostatic pressure induced by the external electric field, which is proportional to E_c^2, the Laplace pressure, proportional to A/r_0, and the electrostatic pressure due to the electric charge, proportional to *B*. Since the both electrostatic pressures act outwards the marble and the Laplace surface-tension pressure inwards, the last term in Eq. (1) should be negative that indeed agrees with the experimental date. For larger marbles, when the Laplace pressure becomes lower than the electrostatic pressure due to the electric charge, the *B* term in Eq. (1) leads to the instability in the so-called Rayleigh limit. According to the present experimental data (Figure 4), the limit radii $r_{0,\mathrm{lim}} = -A/B$ are equal to 3.3 mm for PTFE marbles and 4.6 mm for PVDF marbles. On the other hand, in the cases of lycopodium-coated marble and water droplet, the last term, *B*, turned out to be close to zero that means that these objects did not receive noticeable charge under a DC field.

Taylor has found[35] by solving the problem in the prolate-spheroid-ellipsoid approximation that for a droplet exerted to electric field some dimensionless parameter *T* exists

$$T = E_c \sqrt{\frac{4\pi\varepsilon\varepsilon_0 r_0}{\gamma}}, \quad (2)$$

where γ is the surface tension at the liquid/oil interface, ε_0 is the vacuum permittivity, ε =2.8 is the oil dielectric constant. Parameter *T* determines the critical field (presented here in SI system of units and in the presence of the dielectric medium), and it is equal to 1.63–1.65 in different approximations. The comparison of Eq. (1) and Eq. (2) yields for liquid marbles:

$$\gamma_{eff} = \frac{4\pi\varepsilon\varepsilon_0 A}{T^2}, \quad (3)$$

where γ_{eff} is the effective surface tension at the marble/oil interface, ε =2.8 is the oil dielectric constant, ε_0 is the vacuum permittivity. The measurement data (Figure 4) allow one to extract the values of the constant *A* in Eq. (1) and to obtain effective surface tensions from Eq. (3), which are summarized in Table I. The value of *T* in Eq. (3) was chosen to be equal to 1.7 that is close to the above theoretical values 1.63–1.65 and gives the same surface tension for the water/oil interface as reported in Ref. 36.

The surface tensions at water/oil and effective surface tensions at water/powder/oil interfaces were in parallel measured with the capillary rise method.[37] According to this method, a height of water rise was measured in a vertical glass capillary tube inserted into a marble immersed in the silicon oil. Before measurements, capillary tubes were treated with oxygen plasma in the plasma cleaner PDC-32G (MTI Corporation) for 5 min and filled with distilled water by a contact with a flat water surface. Then the capillary tube was carefully introduced into a 20 µl marble immersed in silicon oil and the additional rise of water pellet in the tube Δh was measured (Figure 5). This additional rise was caused by the Laplace pressure depending on the effective surface tension γ_{eff} at the marble-silicon oil interface and on the radius of a spherical marble r_0 according to

$$\frac{2\gamma_{eff}}{r_0} = \rho g \Delta h . \quad (4)$$

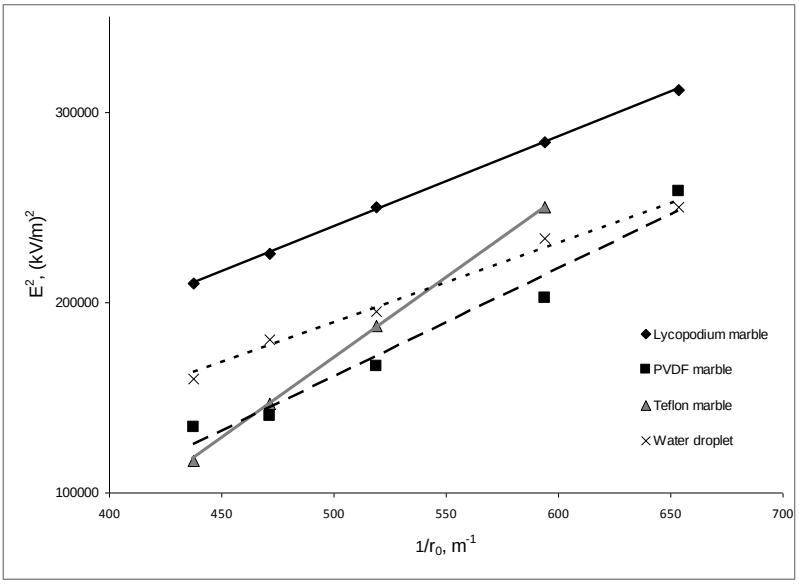

FIG. 4. Squared critical electric field versus inverse radius, $1/r_0$, of the spherical marble of an equivalent volume. Different slopes resemble different surface energies at the marble/oil interfaces.

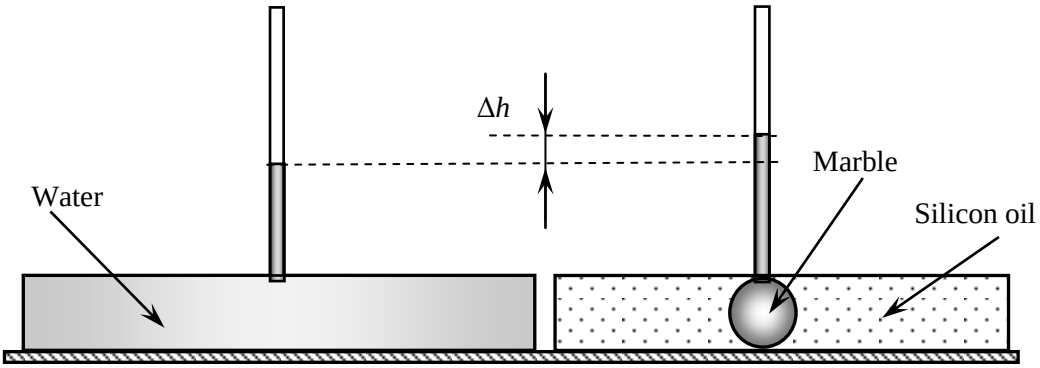

FIG. 5. Scheme of the measurement of surface tension with capillary method.

The densities of water and silicon oil are very close, so the gravity may be neglected. Indeed, shapes of marbles and water droplets were spherical. The surface tensions values calculated according to Eq. (4) are presented in the last column of Table I.

It should be stressed that the surface tensions at water/oil interface of droplets calculated by two methods (Eq. (3) and Eq. (4)) are the same and coincide with the value reported in Ref.36. As is seen from the comparison with the results of the capillary rise method, the critical field method gives reasonable values also for the lycopodium marble. These are just the two cases when B in Eq. (1) is zero that corresponds to uncharged interfaces. The surface tensions for the charged PTFE and PVDF marbles are overestimated since Eqs. (2) and (3) do not take into account the interface charge. The advantage of methods based on the electric field measurement is the intactness of powder interfaces at which the surface tension is determined.

TABLE I. Effective surface tensions at the silicon oil /marble interfaces.

Object	*A* in Eq. (1), $(kV)^2/m$	Surface tensions, mJ/m^2	
		According to Eq. (3) with T=1.7	Capillary rise method
PTFE marble	850.8	92 ± 9	41.4±3.0
PVDF marble	567.2	61 ± 6	42.2±3.3
Lycopodium marble	479.0	52 ± 5	35.2±2.4
Water droplet	381.8	41 ± 4	42.0±2.9

References

1. P. Aussillous and D. Quéré, Nature **411**, 924 (2001).
2. N. Pike, D. Richard, W. Foster, and L. Mahadevan, Proc. R. Soc. London, Ser. B **269**, 1211 (2002).
3. U. K. H. Bangi, S. L. Dhere, and A. Venkateswara Rao, J. Mater. Sci. **45**, 2944 (2010).
4. R. A.Venkateswara, M. M. Kulkarni, and Sh. D. Bhagat, J. Colloid Interface Sci. **285**, 413 (2005).
5. P. Aussillous and D. Quéré, Proc. R. Soc. London, Ser. A **462**, 973 (2006).
6. M. I. Newton, D. L. Herbertson, S. J. Elliott, N. J. Shirtcliffe, and G. J McHale, J. Phys. D **40**, 20 (2007).
7. G. McHale, S. J. Elliott, M. I. Newton, D. L. Herbertson, and K. Esmer, Langmuir **25**, 529 (2009).
8. E. Bormashenko, R. Pogreb, Ye. Bormashenko, A. Musin, and T. Stein, Langmuir **24**, 12119 (2008).
9. E. Bormashenko, R. Pogreb, G. Whyman, A. Musin, Ye. Bormashenko, and Z. Barkay, Langmuir **25**, 1893 (2009).
10. E. Bormashenko, Ye. Bormashenko, A. Musin, and Z. Barkay, ChemPhysChem. **10**, 654 (2009).
11. E. Bormashenko, Ye. Bormashenko, and A. Musin, J. Colloid Interface Sci. **333**, 419 (2009).
12. H.-G. Braun and A. Zamith Cardoso, Colloids Surfaces B, **97**, 43 (2012).
13. P. S. Bhosale, M. V. Panchagnula, and H. A. Stretz, Appl. Phys. Lett. **93**, 034109 (2008).
14. D. Dupin, S. P. Armes, and S. Fujii, J. Am. Chem. Soc. **131**, 5386 (2009).
15. S. Fujii, S. Kameyama, S. P. Armes, D. Dupin, M. Suzaki, and Y. Nakamura**,** Soft Matter **6**, 635 (2010).
16. S. Fujii, M. Aono, S. Suzaki, Sh.-I. Hamasaki, Y. Yusa and Y. Nakamura, Macromolecules **45**, 2863 (2012).
17. Y. Zhao, J. Fang, H. Wang, X. Wang, and T. Lin, Adv. Mater. **22**, 707 (2010).
18. N. Eshtiaghi, J. S .Liu, W. Shen, and K. P. Hapgood, Powder Technol. **196**, 126 (2009).
19. T. Arbatan, L. Li, J. Tian and W. Shen Adv. Healthcare Mater., **1**, 80 (2012).
20. E. Bormashenko, R. Pogreb, G. Whyman, and A. Musin, Colloid Surface A **351**, 78 (2009).
21. M. Dandan and H. Y. Erbil, Langmuir **25,** 8362 (2009).

22. C. Planchette, A. L. Biance and E. Lorenceau, Europhysics Lett., **97**, 14003 (2012).
23. E. Bormashenko, T. Stein, G. Whyman, Ye. Bormashenko, and R. Pogreb, Langmuir **22**, 9982 (2006).
24. E. Bormashenko, Curr. Opin. Colloid Interface Sci. **16**, 266 (2011).
25. G. McHale and M. I. Newton, Soft Matter **7**, 5473 (2011).
26. C. Planchette, A. L. Biance and E. Lorenceau, Europhysics Lett., **97**, 14003 (2012).
27. D. Dupin, K. L. Thompson, and St. P. Armes, Soft Matter **7**, 6797 (2011).
28. C. Aberle, M. Lewis, G. Yu, N. Lei, and J. Xu, Soft Matter **7**, 11314 (2011)
29. E. Bormashenko, R. Balter, and D. Aurbach, Appl. Phys. Lett. **97**, 91908 (2010).
30. E. Bormashenko, Ye. Bormashenko, R. Pogreb, and O. Gendelman, Langmuir **27**, 7 (2011).
31. E. Bormashenko, R. Pogreb, T. Stein, G. Whyman, M. Schiffer, and D. Aurbach, J. Adhesion Sci. Technol. **25**, 1371 (2011).
32. Y. Zhao, Z. Hu, M. Parhizkar, J. Fang, X. Wang and T. Lin, Microfluid Nanofluid., 2012, DOI 10.1007/s10404-012-0976-9.
33. E. Bormashenko, R. Pogreb, R. Balter, O. Gendelman, and D. Aurbach Applied Physics Letters **100**, 151601 (2012).
34. E. Bormashenko, R. Pogreb, A. Musin J. Colloid and Interface Sci. **366,** 196, (2012).
35. G. Taylor Proc. R. Soc. London, Ser. A **280**, 383 (1964).
36. B.P.Binks, J.H. Clint Langmuir **18,** 1270 (2002).
37. T. Arbatan, W. Shen Langmuir **27**, 12923 (2011).